DHODH inhibition represents a therapeutic strategy and improves abiraterone treatment in castration-resistant prostate cancer

Junjian Wang

wangjj87@mail.sysu.edu.cn

Sun Yat-sen University https://orcid.org/0000-0002-5328-2908

guo shaoqiang

Sun Yat-sen University

Miao miaomiao

Sun Yat-sen University

Wu yufeng

Sun Yat-sen University

Wu Qinyan

Sun Yat-sen University

Pan dongyue

Kang Zhanfang

Zeng Jianwen

Chengfei Liu

UC Davis https://orcid.org/0000-0002-2452-8788

Zhong Guoping

Article

Keywords: DHODH, Therapeutic target, CRPC, Androgen biosynthesis

Posted Date: November 25th, 2023

DOI: https://doi.org/10.21203/rs.3.rs-3633354/v1

Additional Declarations: There is **NO** conflict of interest to disclose.

Version of Record: A version of this preprint was published at Oncogene on March 13th, 2024. See the published version at https://doi.org/10.1038/s41388-024-03005-4.

Abstract

Castration-resistant prostate cancer (CRPC) is an aggressive disease with poor prognosis, and there is an urgent need for more effective therapeutic targets to address this challenge. Here, we showed that Dihydroorotate dehydrogenase (DHODH), an enzyme crucial in the pyrimidine biosynthesis pathway, is a promising therapeutic target for CRPC. The transcript levels of DHODH were significantly elevated in prostate tumors and were negatively correlated with the prognosis of patients with prostate cancer. DHODH inhibition effectively suppressed CRPC progression by blocking cell cycle progression and inducing apoptosis. Notably, treatment with BAY2402234 activated androgen biosynthesis signaling in CRPC cells. However, the combination treatment with BAY2402234 and abiraterone decreased intratumoral testosterone levels and induced apoptosis, which inhibited the growth of CWR22Rv1 xenograft tumors and patient-derived xenograft organoids. Taken together, these results establish DHODH as a key player in CRPC and as a potential therapeutic target for advanced prostate cancer.

INTRODUCTION

Prostate cancer is a highly prevalent malignancy among males, with a five-year survival rate of approximately 50% [1, 2]. Initially, most patients present with androgen-dependent prostate cancer, making endocrine therapy targeting the androgen receptor (AR) the primary treatment strategy for castration-resistant prostate cancer (CRPC) [3, 4]. The introduction of novel anti-androgen therapeutic agents, including enzalutamide, abiraterone, and apalutamide, has significantly improved the overall survival rate of patients [5–7]. However, *de novo* and acquired resistance remain a significant challenge. Therefore, there is an urgent need to develop new and effective targeted drugs to overcome these limitations.

The production of pyrimidine nucleotides in organisms primarily occurs through two pathways: the *de novo* synthesis pathway and salvage synthesis pathway [8, 9]. In rapidly proliferating cells, such as tumor cells and T-cells, pyrimidine nucleotides are continuously produced, predominantly through the *de novo* synthesis pathway [10–12]. Dihydroorotate dehydrogenase (DHODH) plays a crucial role in catalyzing the fourth step of the *de novo* pyrimidine synthesis pathway [12]. It oxidizes dihydroorotic acid and converts it to orotate using glutamine as a substrate. Orotate is subsequently converted to UMP via the catalytic activity of UMP synthetase [13, 14].

Initially, various inhibitors targeting DHODH activity were developed for the treatment of autoimmune diseases such as rheumatoid arthritis and multiple sclerosis [15, 16]. In recent years, DHODH inhibitors have shown potent antitumor activities against certain malignant tumors. Some inhibitors such as ASLAN300 have been used in clinical trials [15, 17]. Therefore, it is crucial to investigate the role and mechanism of action of DHODH and its inhibitors in tumors [18–20].

In this study, we observed significant upregulation of DHODH in prostate cancer tumors, indicating its potential role in the disease. Furthermore, we investigated the effects of BAY2402234, a selective inhibitor

of DHODH, on the growth of CRPC cells, both *in vitro* and *in vivo*. Our findings demonstrate that BAY2402234 effectively inhibited the proliferation of CRPC cells by interfering with DNA replication and cell cycle progression, ultimately leading to DNA damage.

Moreover, BAY2402234 treatment upregulated testosterone and dihydrotestosterone levels in prostate cancer cells. This suggested a potential compensatory mechanism in response to DHODH inhibition. Notably, when combined with abiraterone, a commonly used therapeutic agent for prostate cancer, the therapeutic efficacy of BAY2402234 is significantly enhanced.

RESULTS

DHODH overexpression associates with CRPC and is a critical dependency of CRPC cell survival and proliferation.

Given its pivotal role in the development of various cancers, DHODH has emerged as an attractive therapeutic target for cancer treatment. Investigating the function of DHODH in prostate cancer could reveal a novel therapeutic strategy for CRPC. Carbamoyl phosphate synthetase 2, aspartate transcarbamylase, and dihydroorotase (CAD) and DHODH, which catalyze the first three and fourth steps, respectively, play crucial roles in the pyrimidine *de novo* synthesis pathway (Fig. 1A). However, CAD is not considered a druggable target. Therefore, we initially assessed the transcript levels and expression of CAD and DHODH in normal and prostate cancer samples using TCGA database (GSE70768). Compared with prostatic hyperplasia tissues, the transcript levels of CAD and DHODH were significantly elevated in prostate tumors (Fig. 1B). Furthermore, the expression of CAD and DHODH negatively correlated with the prognosis of patients with prostate cancer (Fig. 1C). To delve deeper into the reliance of CRPC growth on *de novo* pyrimidine synthesis, we used siRNA to specifically knockdown CAD and DHODH, resulting in a notable inhibition of cell proliferation in C4-2B and CWR22Rv1 cells (Fig. 1D and E). Indeed, knockdown of DHODH by siRNA induced the expression of c-PARP, c-Caspase3 and c-Caspase7 in prostate cancer cells (Fig. 1F). In addition, DHODH knockout (sgDHODH) suppressed colony formation in C4-2B and CWR22Rv1 cells (Fig. 1G). Collectively, these data suggest that blocking *de novo* pyrimidine synthesis via DHODH inhibition is a promising therapeutic approach for prostate cancer treatment.

DHODH inhibitor inhibits proliferation and survival in CRPC cells.

BAY2402234 is a novel, highly selective, and effective DHODH inhibitor [21]. Given the crucial role of DHODH in prostate cancer, we first investigated whether its inhibitor exerted growth inhibitory effects *in vitro*. The prostate cancer cell lines, LNCaP, C4-2B, CWR22Rv1, and VCaP-CRPC, were treated with different doses of BAY2402234 with or without uridine in FBS. Cell growth was significantly inhibited by BAY2402234 and this inhibition was rescued by supraphysiological uridine (Fig. 2A). Consistent with the findings of the DHODH gene knockdown experiments, treatment of C4-2B and CWR22Rv1 cells with BAY2402234 resulted in reduced colony formation in a dose-dependent manner (Fig. 2B). Further investigation using a 3D organoid model demonstrated that BAY2402234 effectively blocked the growth

and survival of CRPC PDX organoids (Fig. 2C and D). Taken together, these results indicate that BAY2402234 suppresses the proliferation and growth of CRPC cells by inhibiting DHODH activity.

DHODH inhibition induces DNA damage, blocks the cell cycle and DNA replication in CRPC cells.

To further investigate the gene programs affected by DHODH inhibition, we conducted an RNA sequencing analysis of C4-2B cells treated with BAY2402234. We performed gene set enrichment analysis (GSEA) to identify transcripts commonly regulated by BAY2402234 at two different doses (Fig. 3A). Our analysis revealed that DNA replication and cell cycle processes were the most down-regulated pathways affected by BAY2402234. Additionally, we observed upregulation of pathways related to p53 signaling, apoptosis, and DNA damage (Fig. 3B and C). GSEA focusing on the cell cycle and DNA replication signaling pathways demonstrated that BAY2402234 significantly inhibited these processes in C4-2B cells (Fig. 3D). At the individual gene level, we confirmed the downregulation of genes involved in the cell cycle (CDC6, CDC45, and CDC25A) and DNA replication pathway (EXO1, UHRF1, and PLK4) upon treatment with BAY2402234. Furthermore, we observed the upregulation of genes in the DNA damage pathway (GADD45A, CLU, and PLK2) following BAY2402234 treatment (Fig. 3E). To validate our findings, we performed quantitative real-time PCR (qRT-PCR) on the target genes identified through GSEA (Fig. 3F). Taken together, BAY2402234 inhibits prostate cancer progression by upregulating the p53 signaling pathway and inducing apoptosis and DNA damage, while DHODH blocks the cell cycle and DNA replication.

DHODH inhibitor exerts potent anti-tumor activity in CRPC in vitro and in vivo.

The significant effect of DHODH inhibition on p53 signaling and induction of apoptosis pathway-related gene programs prompted us to investigate whether DHODH controls the expression of apoptosis markers. Indeed, treatment with BAY2402234 induced the expression of c-PARP, c-Caspase3 and c-Caspase7 in a dose-dependent manner in both C4-2B and CWR22Rv1 cells (Fig. 4A). These findings were further confirmed using flow cytometry (Fig. 4B). Given the essential role of pyrimidines in DNA replication, we evaluated the levels of DNA replication-related genes. BAY2402234 significantly suppressed the mRNA expression of PLK4, BRCA1, EXO1, UHRF1, and CHEK1 (Fig. 4C). To further assess the potential *in vivo* effects of BAY2402234, we established a CWR22Rv1 xenograft mouse model. Oral administration of BAY2402234 (5mg/Kg) effectively suppressed tumor growth (Fig. 4D). Histological examination of tumor tissue sections using H&E staining revealed morphological changes in tumor cells in the treatment group. Additionally, immunohistochemical staining for Ki67 and c-Caspase3 demonstrated that BAY2402234 strongly inhibited prostate tumor cell proliferation and induced apoptosis (Fig. 4E). All the *in vivo* pharmacodynamic results were consistent with our *in vitro* findings.

DHODH inhibition activates intracrine androgen biosynthesis pathway and AR signaling.

Our data suggest that the inhibition of DHODH activity could significantly inhibit the proliferation of CRPC. Interestingly, GSEA showed that BAY2402234 may activate the lipid metabolism pathway in C4-2B cells (Fig. 5A). At the individual gene level, we observed the upregulation of genes involved in androgen

biosynthesis in BAY2402234 treated cells. Further analysis of this pathway revealed that BAY2402234 upregulated the expression of individual genes involved in the androgen synthesis in C4-2B cells, including Hydroxy-Delta-5-Steroid Dehydrogenase, 3 Beta- And Steroid Delta-Isomerase 1 (HSD3B1) and Aldo-Keto Reductase Family 1 Member C3 (AKR1C3) (Fig. 5B and C). To validate RNA-seq analysis, qRT-PCR was performed on BAY2402234-treated C4-2B and VCaP-CRPC cells. These results confirmed the upregulation of the androgen biosynthesis genes (Fig. 5D). To investigate whether BAY2402234 directly affects androgen synthesis in CRPC cells, testosterone (T), and dihydrotestosterone (DHT) levels were measured in VCaP-CRPC and CWR22Rv1 cells after treatment with BAY2402234, using LC-MS/MS. These results suggest an increase in testosterone and DHT levels (Fig. 5E). Furthermore, BAY2402234 upregulated the AR signaling pathway (Fig. S1A and B). These data suggest that, although BAY2402234 can suppress the CRPC tumor growth, it may activate to AR signaling and eventually reduce the efficacy.

Combine DHODH inhibitor and abiraterone treatment adds sensitivity of CRPC inhibition and blocks intracrine androgen.

Abiraterone is a cytochrome P450 family 17 subfamily A member 1 (CYP17A1) inhibitor that is primarily used in combination with prednisone for the treatment of metastatic CRPC and serves as a key drug in clinical prostate cancer treatment [22, 23]. By suppressing CYP17A1, abiraterone effectively blocks androgen production and AR signaling, thereby inhibiting the progression of prostate cancer [24, 25]. To eliminate the unwanted effects of AR signaling activation by BAY2402234, we further evaluated the combination treatment of BAY2402234 and abiraterone in CRPC cells. Our results demonstrate that the combination of BAY2402234 and abiraterone effectively enhanced the inhibition of cell proliferation (Fig. 6A) and induced apoptosis (Fig. 6B and S2A). Further experiments using 3D organoids confirmed the findings (Fig. 6C). Through RNA-seq and qRT-PCR analyses, we observed that BAY2402234 significantly upregulated AKR1C3, a key enzyme involved in androgen synthesis [26]. Subsequently, we treated VCaP-CRPC and CWR22Rv1 cells with the AKR1C3 inhibitor, indomethacin in combination with BAY2402234. The experimental results demonstrated that this combination effectively inhibited CRPC cell proliferation and induced apoptosis (Fig. S2B and C). Moreover, we conducted siRNA transfection to knockdown AR expression in C4-2B and CWR22Rv1 cells, followed by treatment with BAY2402234. The combination of AR knockdown and BAY2402234 treatment significantly suppressed CRPC cell proliferation (Fig. 6D and E). In addition, we used a CWR22Rv1 xenograft model to evaluate the potential enhancement of BAY2402234 treatment with abiraterone *in vivo*. BAY2402234 alone effectively inhibited tumor growth, and when combined with abiraterone, further inhibition of tumor growth was observed (Fig. 6F-H). Testosterone levels were measured in the tumor tissues using LC-MS/MS. The results showed that BAY2402234 insignificantly increased testosterone levels, and abiraterone suppressed testosterone level in tumor tissue compared to those in the control group. When abiraterone was combined with BAY2402234, the testosterone levels in the tumor were drastically reduced (Fig. 6I). H&E staining of tumor tissue sections revealed significant expansion of the intercellular space and necrosis of tumor cells. Immunohistochemical Ki67 and c-Caspase3 staining demonstrated that BAY2402234 strongly inhibited the proliferation of cancer cells (Fig. S2D). In summary, our results indicate that BAY2402234 effectively

inhibited CRPC tumor growth in vivo by targeting DHODH activity, and when combined with abiraterone, it further enhanced the inhibition of tumor growth.

DISCUSSION

Prostate cancer, a common malignancy in men, is predominantly managed through endocrine therapy at advanced stages [27]. The inclusion of next-generation androgen-targeting agents, enzalutamide, abiraterone, apalutamide, and darolutamide, in advanced prostate cancer treatment guidelines has significantly increased patient survival rates [28, 29]. However, a persistent challenge arises in the form of eventual tumor cell resistance after the initial effective treatment phase [30]. Hence, the exploration of novel therapeutic targets and strategies is of paramount importance to overcome the limitations of endocrine therapy.

Pyrimidine, a pivotal substrate for DNA replication and synthesis, plays a fundamental role in the *de novo* pyrimidine synthesis pathway [14, 31]. This pathway plays a crucial role in the proliferation and development of malignant tumors. Of particular interest is DHODH, an enzyme involved in *de novo* pyrimidine biosynthesis, which has gained substantial attention as a promising target for cancer therapy [32, 33]. As a key catalyst in *de novo* pyrimidine biosynthesis, DHODH orchestrates the conversion of dihydroorotate to orotate through dehydration reactions [34].

A range of DHODH inhibitors, including MLS930 and brequinar, have demonstrated potential anticancer activities [35]. Certain agents, such as RP7214, have even secured Food and Drug Administration (FDA) approval for the treatment of acute myeloid leukemia [36–38]. In this study, we established DHODH as an attractive therapeutic target for prostate cancer treatment. Notably, the DHODH inhibitor BAY2402234 exhibited pronounced inhibition of prostate cancer cell proliferation and survival, both *in vitro* and *in vivo*.

In this study, we investigated the underlying mechanism of DHODH inhibition in suppressing of prostate cancer development. RNA-seq analyses revealed that BAY2402234 downregulated the DNA replication signaling pathway and induced G1/S cell cycle arrest in prostate cancer cells. These findings were further corroborated by qRT-PCR assays. Moreover, targeted knockdown or specific inhibition of DHODH has been shown to induce apoptosis in prostate cancer cells.

Prostate cancer progression is closely associated with AR expression and androgen levels. Intratumoral androgens contribute notably to CRPC [39, 40]. Androgen biosynthetic enzymes, including CYP11A1, CYP17A1, AKR1C3, and HSD3Bs, mediate androgen synthesis via both classical and backdoor pathways [41, 42]. Surprisingly, our C4-2B RNA-seq analysis revealed an unanticipated upregulation of various androgen synthases, such as CYP11A1, AKR1C3, and HSD17Bs, upon exposure to BAY2402234 [43, 44]. This observation was further substantiated by quantifying androgen levels in prostate cancer cell lines using LC-MS/MS, which aligned with the aforementioned trends.

Furthermore, augmented androgen biosynthesis within tumors has the potential to reactivate AR signaling in CRPC. This notion was reinforced by subsequent GSEA, which demonstrated that

BAY2402234 enhances the AR signaling pathway in C4-2B cells. Consequently, while DHODH inhibitors exhibit heightened anticancer efficacy against prostate cancer, the concurrent upregulation of androgen levels may inadvertently attenuate their anti-prostate cancer functionality. Importantly, previous studies on DHODH have predominantly focused on its role in *de novo* pyrimidine synthesis within the inner mitochondrial membrane [12]. However, the broad impact of these inhibitors on androgen synthase expression in prostate cancer, thereby modulating androgen synthesis, provides a novel avenue for exploring the multifaceted functions of DHODH.

In the spectrum of androgen deprivation therapy (ADT) for prostate cancer, abiraterone targets CYP17A1, resulting in reduced testosterone levels [45]. Drawing on this mechanistic insight, we hypothesized that a combined therapeutic approach using BAY2402234 and abiraterone would yield synergistic effects. While BAY2402234 induces apoptosis through inhibition of DNA replication, abiraterone complements this effect by curbing prostate cancer progression via suppression of elevated androgen levels. Rigorous *in vitro* and *in vivo* experiments validated the efficacy of dual-drug combinations, with additional enhancement observed when indomethacin, an AKR1C3 activity inhibitor, was integrated with BAY2402234.

MATERIALS AND METHODS

Cell culture and organoid culture

HEK293T, C4-2B, LNCaP, and CWR22Rv1 cells were obtained from the American Type Culture Collection (ATCC, Manassas, VA, USA). All cell line experiments were performed within six months of receipt from the ATCC or resuscitation after cryopreservation. VCaP-CRPC was a kind gift from Professor Hongwu Chen (Department of Biochemistry and Molecular Medicine, School of Medicine, University of California, Davis, California, USA). HEK293T and VCaP-CRPC cells were cultured in DMEM supplemented with 10% (fetal bovine serum FBS (Gibco, Germany) and 1% penicillin/streptomycin (Gibco). The other cell lines were maintained in RPMI-1640 supplemented with 10% fetal bovine serum (FBS) (Gibco) and 1% penicillin/streptomycin (Gibco). All cell lines were routinely tested as mycoplasma-free by PCR and authenticated using the short tandem repeat (STR) method. All cells were cultured at 37℃ in a humidified incubator with 5% CO_2.

Organoids were cultured from PDX xenografts when the tumor size reached approximately 500mm^3. Briefly, the dissected tumor was finely minced and transferred into a 50 mL conical tube, including a digestive mixture consisting of serum-free DMEM / F-12 medium (Gibco) and 1 mg / mL collagenase IV (Sigma-Aldrich, Germany), and incubated at 37 °C for 40 min. Isolated organoids were mixed with 5μL Matrigel (BD Biosciences, USA) and inoculated into a 96-well plate. The culture medium contained phenol red-free DMEM/F12 (Gibco) supplemented with penicillin/streptomycin/glutamine (100 mg/mL) (Gibco), HEPES (10 mM) (Sigma-Aldrich), Pen-strep (1×) (Gibco), Y-27632 (10 μM) (Selleck, USA), SB202190 (10 μM) (Sigma-Aldrich) FGF 10 (10 ng/mL) (Peprotech, USA), FGF 2 (5 ng/mL) (Peprotech), R-Spondin 1 (250 ng/mL), Noggin (100ng/ml) (Peprotech), BSA (0.1%) (Beyotime, China), A8301 (500 nM) (Tocris

Bioscience, UK), EGF (5 ng/mL) (Peprotech), N-acetylcysteine (1.25 μM) (Sigma-Aldrich), nicotinamide (5 mM) (Sigma-Aldrich), B27 supplement (1×) (Invitrogen, Germany), DHT (1 nM) (Selleck), and 100μL of supplemented culture medium were added per well, and organoids were maintained in a 37 °C humidified atmosphere under 5% CO2. For the patient-derived xenograft, PDX-TM (JAX ID: TM00298) was purchased form the Jackson Laboratory (USA).

Chemicals Sources

Sources for chemicals are as follows: BAY2402234 (BAY, purity >99%) were synthesized by WuXi AppTec (China). Uridine was obtained from TargetMol (Cat#T2221) (USA). Abiraterone was obtained from MCE (Cat# HY70013) (USA). Indomethacin was purchased from Selleck (Cat#S1723).

siRNA transfection and lentivirus infection

siRNA transfection was performed using Dharmafectin#1 (Dharmacon, USA) and Opti-MEM (Invitrogen), following the manufacturer's instructions. Lentiviral production was performed in HEK293T cells, as described in our previous study. [46] Primers for DHODH and CAD are shown in Supplementary Table S1.

Colony formation

Five hundred cells per well were plated in 6-well plates, treated with varying concentrations of BAY2402234, and maintained for 10-14 days. The medium was changed every three days. The colonies were fixed with 4% paraformaldehyde for 20 min. Colonies were washed with PBS after staining with crystal violet for 20 min and the number of colonies was counted.

Flow cytometry and FACS

The cells were collected and filtered through a 40-μm nylon cell strainer. The cells were washed with PBS and resuspended in binding buffer with Annexin V-FITC (Wanleibio, China) and Propidium Iodide (Wanleibio) at 4℃ for 15min and acquired on a FACS on CytoFLEX S (BECKMAN COULTER, USA). Data were analyzed using software (CytExpert 2.3).

Organoid viability

For organoid viability, organoids were suspended in media with Matrigel (10:1) and seeded in 96-well plates at 300-500 organoids per well. After 12h, a series of diluted compounds was added to 100μL of media and added to the organoids. After 6 days of incubation, Cell-Titer Glo reagent (Promega, USA) was added to measure the luminescence. The data are expressed as the percentage of living cells, and the solvent-treated cells were set to 100. After 6 days of culture, the medium was carefully drawn, 100μL of live / dead reagent (EVERBRIGHT, USA) was added and incubated at room temperature for 30 min. The green fluorescent precursor compound Calcein Am (494 / 517 nm) represented living cells, and Propidium (528 / 617 nm) represented dead cells. The above experiments were repeated three times.

RNA sequencing (RNA-seq)

C4-2B cells were treated with vehicle (DMSO) or BAY2402234(25nM or 50nM) for 48 h before RNA extraction. RNA-seq libraries from 1μg of total RNA were prepared using Illumina Tru-seq RNA sample, according to the manufacturer's instructions. The RNA Sequence libraries were validated using the MIGSEQ2000 SE50 system (BGI Tech, Wuhan, China). FASTQ-formatted sequence data were analyzed using a standard BWA-Bowtie-Cufflinks workflow[47-49]. Briefly, sequence reads were mapped to the reference human genome assembly (GRCh37/hg19) using BWA and Bowtie 2. Subsequently, the Cufflinks package[50] was used for transcript assembly, quantification of normalized gene and isoform expression in fragments per kilobase of exon model per million mapped reads (FPKM), and testing for differential expression (Cuffdiff). To avoid spurious fold levels due to low expression values, only those genes with expression FPKM values >1 for both the control cells and the BAY2402234 treated cells were included. Changes in expression ≥ 1.5 folds (increase or decrease) were chosen. Gene Set Enrichment Analysis (http://metascape.org/gp/index.html#/main/step1) was used to rank the genes based on the shrunken limma log2 fold changes. The cluster was displayed with R statistical package (http://www.rproject.org/). Signaling pathways were analyzed by KEGG and hallmark databases, and displayed with SangerBox (http://sangerbox.com/tool.html) in the form of bubble map.

Gene Set Enrichment Analysis (GSEA)

GSEA was performed with the Java desktop software (http://www.broadinstitute.org/gsea) as described previously [51]. Gene were ranked according to the shrunken limma $\log^2$ fold change, and the GSEA tool was used in 'pre-ranked' model with all default parameters. The GOBP-DNA replication, GOBP-cell cycle pathway and HALLMARK-androgen response pathways were used in the GSEA analysis.

Analysis of CAD and DHODH mRNA expression and association with survival in clinical tumors.

Publicly available prostate cancer expression datasets GSE70768 from a previous study were downloaded from GEO (https://www.ncbi.nlm.nih.gov/geo/). The normalized probe set expression for CAD and DHODH was compared between the two groups by a two-tailed t test for significance.[52] Computations were conducted in R statistical package (http://www.rproject.org/). CAD and DHODH expression associations with survival analysis were performed in prostate adenocarcinoma patients from GEPIA 2 (http://gepia2.cancer-pku.cn/).

Quantitative real-time PCR (qRT-PCR) and Western blotting (WB)

Total RNA was isolated using TRIzol (Invitrogen) reagent. cDNA was prepared, amplified, and measured in the presence of SYBR as previously described. Melting curve analysis was performed before fluorescence values were collected. Cell lysates were analyzed by western blotting using antibodies that specifically recognize the designated proteins. The PCR primers and antibodies used in this study are listed in the Supplementary Tables S2 and S3.

In vivo tumorigenesis assay

The animal experiments were approved by the Committee for Ethics of Animal Experimentation and conducted in accordance with the guidelines for animal experiments at Sun Yat-sen University. Four-week-old BALB/C nude mice were purchased from Sun Yat-sen University Laboratory Animal Center (Guangzhou, China). CWR22Rv1 cells (4×10^6) were mixed with Matrigel and PBS (1:1) and injected subcutaneously into the flank of nude mice. when the tumor size reached approximately 50 mm^3. The mice were randomly divided into the indicated groups. The mice were treated intraperitoneally (i.p.) with 100μL of either vehicle (DMSO) or abiraterone (0.5 mmol/kg), or performed oral gavage BAY2402234 (25 mg/Kg) for 18-21 days. Tumor volumes and body weights were measured every 2 days. Tumor tissues were harvested, weighed, and evaluated by immunohistochemistry.

Immunohistochemistry (IHC) staining

Tumors were fixed in formalin and paraffin-embedded tissue blocks were dewaxed, rehydrated, and blocked for endogenous peroxidase activity. Antigen retrieval was performed in sodium citrate buffer (0.01 mol/L, pH6.0 or pH8.0) (Servicebio, China) in a microwave oven at 1000 W for 20 min and then at 100 W for 20 min. Non-specific antibody binding was blocked by incubation with goat serum for 30 min at room temperature. slides were then incubated with antibody at 4℃ overnight. The slides were subsequently washed with PBS and incubated with secondary antibody for 30 min. The sections were stained with DAB (Servicebio) and hematoxylin (Servicebio). The slides were dehydrated and sealed with a neutral resin. The antibodies used in this study are listed in the Supplementary Table S3. The Immunohistochemical kit in this study are from Servicebio (Cat# G1215-200T).

Sample preparation and androgen measurement

Androgen levels in the cells were measured using ultra-high-performance liquid chromatography coupled with electrospray ionization tandem mass spectrometry (UPLC-MS/MS). To assess the effect of BAY2402234 on the expression of dihydrotestosterone (DHT) and testosterone (T), cells were treated with either BAY2402234 or DMSO (vehicle control). The cells were cultured in phenol red-free medium with charcoal-dextran-stripped stripped FBS for 72 h before androgen measurement. Ultrapure water was used to lyse the cultured cells and the extracts were obtained using acetonitrile. The samples were then analyzed using an Agilent 1290 LC and Agilent 6460 Triple Quadrupole LC/MS system (AB Sciex, USA), with ions monitored at 289.4 > 109.2 for T and 291.2 > 255.4 for DHT.

Statistical analysis

All analyses were performed using GraphPad Prism 7 software (GraphPad Software, USA). The experimental data are expressed as the means ± standard deviation (SD) of at least three independent experiments. The degree of vibration within each dataset is depicted as SD in each figure. A two-tailed unpaired Student 's t-test was used for to determine statistical significance between two groups. All statistical tests were justified as appropriate and the data met the assumptions of normal distribution. $p < 0.05$ was considered to indicate statistically significant differences (*P < 0.05; ** $p < 0.01$, *** $p < 0.005$, **** $p < 0.0001$). Sample size was not predetermined using a specific statistical method.

Declarations

FINANCIAL SUPPORT: This research was supported by the National Natural Science Foundation of China (82273956), the Guangdong Basic and Applied Basic Research Foundation (2022B1515130008), the Key Research and Development Plan of Guangzhou City (202206080007), and Science and Technology Planning Project of Guangdong Province (2023A0505010013).

AUTHOR CONTRIBUTIONS: JJW, CFL, and GPZ conceived of and designed the experiments. SQG, MMM, YFW, and QYW performed the experiments and collected data. DYP and ZFK performed the bioinformatics analysis. SQG, JWZ, JJW and CFL wrote and edited the manuscript. All authors agree with the published version of the manuscript.

ACKNOWLEDGMENTS: We thank the Laboratory Animal Center of Sun Yat-sen University for providing the technologies equipment.

COMPENTING INTERESTS: The authors declare no competing financial interests.

DATA AVAILABILITY

The data obtained in this study are available upon reasonable request from the corresponding authors.

References

1. Desai K, McManus JM, Sharifi N. Hormonal Therapy for Prostate Cancer. *Endocrine reviews* 2021; 42: 354-373.
2. Smith MR, Hussain M, Saad F, Fizazi K, Sternberg CN, Crawford ED *et al*. Darolutamide and Survival in Metastatic, Hormone-Sensitive Prostate Cancer. *The New England journal of medicine* 2022; 386: 1132-1142.
3. Auchus RJ, Sharifi N. Sex Hormones and Prostate Cancer. *Annual review of medicine* 2020; 71: 33-45.
4. Hankey W, Chen Z, Wang Q. Shaping Chromatin States in Prostate Cancer by Pioneer Transcription Factors. *Cancer research* 2020; 80: 2427-2436.
5. Armstrong AJ, Szmulewitz RZ, Petrylak DP, Holzbeierlein J, Villers A, Azad A *et al*. ARCHES: A Randomized, Phase III Study of Androgen Deprivation Therapy With Enzalutamide or Placebo in Men With Metastatic Hormone-Sensitive Prostate Cancer. *Journal of clinical oncology : official journal of the American Society of Clinical Oncology* 2019; 37: 2974-2986.
6. Chi KN, Chowdhury S, Bjartell A, Chung BH, Pereira de Santana Gomes AJ, Given R *et al*. Apalutamide in Patients With Metastatic Castration-Sensitive Prostate Cancer: Final Survival Analysis of the Randomized, Double-Blind, Phase III TITAN Study. *Journal of clinical oncology : official journal of the American Society of Clinical Oncology* 2021; 39: 2294-2303.

7. Vellky JE, Ricke WA. Development and prevalence of castration-resistant prostate cancer subtypes. *Neoplasia (New York, NY)* 2020; 22: 566-575.
8. Löffler M, Fairbanks LD, Zameitat E, Marinaki AM, Simmonds HA. Pyrimidine pathways in health and disease. *Trends in molecular medicine* 2005; 11: 430-437.
9. Nakashima A, Kawanishi I, Eguchi S, Yu EH, Eguchi S, Oshiro N *et al*. Association of CAD, a multifunctional protein involved in pyrimidine synthesis, with mLST8, a component of the mTOR complexes. *Journal of biomedical science* 2013; 20: 24.
10. Koundinya M, Sudhalter J, Courjaud A, Lionne B, Touyer G, Bonnet L *et al*. Dependence on the Pyrimidine Biosynthetic Enzyme DHODH Is a Synthetic Lethal Vulnerability in Mutant KRAS-Driven Cancers. *Cell chemical biology* 2018; 25: 705-717.e711.
11. Scherer S, Oberle SG, Kanev K, Gerullis AK, Wu M, de Almeida GP *et al*. Pyrimidine de novo synthesis inhibition selectively blocks effector but not memory T cell development. *Nature immunology* 2023; 24: 501-515.
12. Madak JT, Bankhead A, 3rd, Cuthbertson CR, Showalter HD, Neamati N. Revisiting the role of dihydroorotate dehydrogenase as a therapeutic target for cancer. *Pharmacology & therapeutics* 2019; 195: 111-131.
13. Villa E, Ali ES, Sahu U, Ben-Sahra I. Cancer Cells Tune the Signaling Pathways to Empower de Novo Synthesis of Nucleotides. *Cancers* 2019; 11.
14. Robinson AD, Eich ML, Varambally S. Dysregulation of de novo nucleotide biosynthetic pathway enzymes in cancer and targeting opportunities. *Cancer letters* 2020; 470: 134-140.
15. Zhou Y, Tao L, Zhou X, Zuo Z, Gong J, Liu X *et al*. DHODH and cancer: promising prospects to be explored. *Cancer & metabolism* 2021; 9: 22.
16. Bar-Or A, Pachner A, Menguy-Vacheron F, Kaplan J, Wiendl H. Teriflunomide and its mechanism of action in multiple sclerosis. *Drugs* 2014; 74: 659-674.
17. Zhou J, Yiying Quah J, Ng Y, Chooi JY, Hui-Min Toh S, Lin B *et al*. ASLAN003, a potent dihydroorotate dehydrogenase inhibitor for differentiation of acute myeloid leukemia. *Haematologica* 2020; 105: 2286-2297.
18. Mao C, Liu X, Zhang Y, Lei G, Yan Y, Lee H *et al*. DHODH-mediated ferroptosis defence is a targetable vulnerability in cancer. *Nature* 2021; 593: 586-590.
19. Pal S, Kaplan JP, Nguyen H, Stopka SA, Savani MR, Regan MS *et al*. A druggable addiction to de novo pyrimidine biosynthesis in diffuse midline glioma. *Cancer cell* 2022; 40: 957-972.e910.
20. Gwynne WD, Suk Y, Custers S, Mikolajewicz N, Chan JK, Zador Z *et al*. Cancer-selective metabolic vulnerabilities in MYC-amplified medulloblastoma. *Cancer cell* 2022; 40: 1488-1502.e1487.
21. Christian S, Merz C, Evans L, Gradl S, Seidel H, Friberg A *et al*. The novel dihydroorotate dehydrogenase (DHODH) inhibitor BAY 2402234 triggers differentiation and is effective in the treatment of myeloid malignancies. *Leukemia* 2019; 33: 2403-2415.

22. Fizazi K, Foulon S, Carles J, Roubaud G, McDermott R, Fléchon A *et al*. Abiraterone plus prednisone added to androgen deprivation therapy and docetaxel in de novo metastatic castration-sensitive prostate cancer (PEACE-1): a multicentre, open-label, randomised, phase 3 study with a 2 × 2 factorial design. *Lancet (London, England)* 2022; 399: 1695-1707.
23. Annala M, Vandekerkhove G, Khalaf D, Taavitsainen S, Beja K, Warner EW *et al*. Circulating Tumor DNA Genomics Correlate with Resistance to Abiraterone and Enzalutamide in Prostate Cancer. *Cancer discovery* 2018; 8: 444-457.
24. Mostaghel EA, Marck BT, Plymate SR, Vessella RL, Balk S, Matsumoto AM *et al*. Resistance to CYP17A1 inhibition with abiraterone in castration-resistant prostate cancer: induction of steroidogenesis and androgen receptor splice variants. *Clinical cancer research : an official journal of the American Association for Cancer Research* 2011; 17: 5913-5925.
25. Ferraldeschi R, Sharifi N, Auchus RJ, Attard G. Molecular pathways: Inhibiting steroid biosynthesis in prostate cancer. *Clinical cancer research : an official journal of the American Association for Cancer Research* 2013; 19: 3353-3359.
26. Asangani I, Blair IA, Van Duyne G, Hilser VJ, Moiseenkova-Bell V, Plymate S *et al*. Using biochemistry and biophysics to extinguish androgen receptor signaling in prostate cancer. *The Journal of biological chemistry* 2021; 296: 100240.
27. Swami U, McFarland TR, Nussenzveig R, Agarwal N. Advanced Prostate Cancer: Treatment Advances and Future Directions. *Trends in cancer* 2020; 6: 702-715.
28. Teo MY, Rathkopf DE, Kantoff P. Treatment of Advanced Prostate Cancer. *Annual review of medicine* 2019; 70: 479-499.
29. Gillessen S, Armstrong A, Attard G, Beer TM, Beltran H, Bjartell A *et al*. Management of Patients with Advanced Prostate Cancer: Report from the Advanced Prostate Cancer Consensus Conference 2021. *European urology* 2022; 82: 115-141.
30. Shore N, Zurth C, Fricke R, Gieschen H, Graudenz K, Koskinen M *et al*. Evaluation of Clinically Relevant Drug-Drug Interactions and Population Pharmacokinetics of Darolutamide in Patients with Nonmetastatic Castration-Resistant Prostate Cancer: Results of Pre-Specified and Post Hoc Analyses of the Phase III ARAMIS Trial. *Targeted oncology* 2019; 14: 527-539.
31. Diehl FF, Miettinen TP, Elbashir R, Nabel CS, Darnell AM, Do BT *et al*. Nucleotide imbalance decouples cell growth from cell proliferation. *Nature cell biology* 2022; 24: 1252-1264.
32. Yang C, Zhao Y, Wang L, Guo Z, Ma L, Yang R *et al*. De novo pyrimidine biosynthetic complexes support cancer cell proliferation and ferroptosis defence. *Nature cell biology* 2023; 25: 836-847.
33. Ma Y, Zhu Q, Wang X, Liu M, Chen Q, Jiang L *et al*. Synthetic lethal screening identifies DHODH as a target for MEN1-mutated tumor cells. *Cell research* 2022; 32: 596-599.
34. Scott LJ. Teriflunomide: A Review in Relapsing-Remitting Multiple Sclerosis. *Drugs* 2019; 79: 875-886.
35. Olsen TK, Dyberg C, Embaie BT, Alchahin A, Milosevic J, Ding J *et al*. DHODH is an independent prognostic marker and potent therapeutic target in neuroblastoma. *JCI insight* 2022; 7.

36. Madak JT, Cuthbertson CR, Chen W, Showalter HD, Neamati N. Design, Synthesis, and Characterization of Brequinar Conjugates as Probes to Study DHODH Inhibition. *Chemistry (Weinheim an der Bergstrasse, Germany)* 2017; 23: 13875-13878.
37. Miyazaki Y, Inaoka DK, Shiba T, Saimoto H, Sakura T, Amalia E *et al*. Selective Cytotoxicity of Dihydroorotate Dehydrogenase Inhibitors to Human Cancer Cells Under Hypoxia and Nutrient-Deprived Conditions. *Frontiers in pharmacology* 2018; 9: 997.
38. Ladds M, van Leeuwen IMM, Drummond CJ, Chu S, Healy AR, Popova G *et al*. A DHODH inhibitor increases p53 synthesis and enhances tumor cell killing by p53 degradation blockage. *Nature communications* 2018; 9: 1107.
39. Cheng Q, Butler W, Zhou Y, Zhang H, Tang L, Perkinson K *et al*. Pre-existing Castration-resistant Prostate Cancer-like Cells in Primary Prostate Cancer Promote Resistance to Hormonal Therapy. *European urology* 2022; 81: 446-455.
40. He Y, Wei T, Ye Z, Orme JJ, Lin D, Sheng H *et al*. A noncanonical AR addiction drives enzalutamide resistance in prostate cancer. *Nature communications* 2021; 12: 1521.
41. Zhou J, Wang Y, Wu D, Wang S, Chen Z, Xiang S *et al*. Orphan nuclear receptors as regulators of intratumoral androgen biosynthesis in castration-resistant prostate cancer. *Oncogene* 2021; 40: 2625-2634.
42. Hearn JWD, Sweeney CJ, Almassi N, Reichard CA, Reddy CA, Li H *et al*. HSD3B1 Genotype and Clinical Outcomes in Metastatic Castration-Sensitive Prostate Cancer. *JAMA oncology* 2020; 6: e196496.
43. Audet-Walsh É, Bellemare J, Lacombe L, Fradet Y, Fradet V, Douville P *et al*. The impact of germline genetic variations in hydroxysteroid (17-beta) dehydrogenases on prostate cancer outcomes after prostatectomy. *European urology* 2012; 62: 88-96.
44. Xu Z, Ma T, Zhou J, Gao W, Li Y, Yu S *et al*. Nuclear receptor ERRα contributes to castration-resistant growth of prostate cancer via its regulation of intratumoral androgen biosynthesis. *Theranostics* 2020; 10: 4201-4216.
45. Liu C, Armstrong CM, Lou W, Lombard A, Evans CP, Gao AC. Inhibition of AKR1C3 Activation Overcomes Resistance to Abiraterone in Advanced Prostate Cancer. *Molecular cancer therapeutics* 2017; 16: 35-44.
46. Huang JL, Yan XL, Li W, Fan RZ, Li S, Chen J *et al*. Discovery of Highly Potent Daphnane Diterpenoids Uncovers Importin-β1 as a Druggable Vulnerability in Castration-Resistant Prostate Cancer. *Journal of the American Chemical Society* 2022; 144: 17522-17532.
47. Langmead B, Trapnell C, Pop M, Salzberg SL. Ultrafast and memory-efficient alignment of short DNA sequences to the human genome. *Genome biology* 2009; 10: R25.
48. Li H, Durbin R. Fast and accurate long-read alignment with Burrows-Wheeler transform. *Bioinformatics (Oxford, England)* 2010; 26: 589-595.
49. Trapnell C, Roberts A, Goff L, Pertea G, Kim D, Kelley DR *et al*. Differential gene and transcript expression analysis of RNA-seq experiments with TopHat and Cufflinks. *Nature protocols* 2012; 7:

562-578.

50. Trapnell C, Williams BA, Pertea G, Mortazavi A, Kwan G, van Baren MJ *et al*. Transcript assembly and quantification by RNA-Seq reveals unannotated transcripts and isoform switching during cell differentiation. *Nature biotechnology* 2010; 28: 511-515.
51. Subramanian A, Tamayo P, Mootha VK, Mukherjee S, Ebert BL, Gillette MA *et al*. Gene set enrichment analysis: a knowledge-based approach for interpreting genome-wide expression profiles. *Proceedings of the National Academy of Sciences of the United States of America* 2005; 102: 15545-15550.
52. Ross-Adams H, Lamb AD, Dunning MJ, Halim S, Lindberg J, Massie CM *et al*. Integration of copy number and transcriptomics provides risk stratification in prostate cancer: A discovery and validation cohort study. *EBioMedicine* 2015; 2: 1133-1144.

Figures

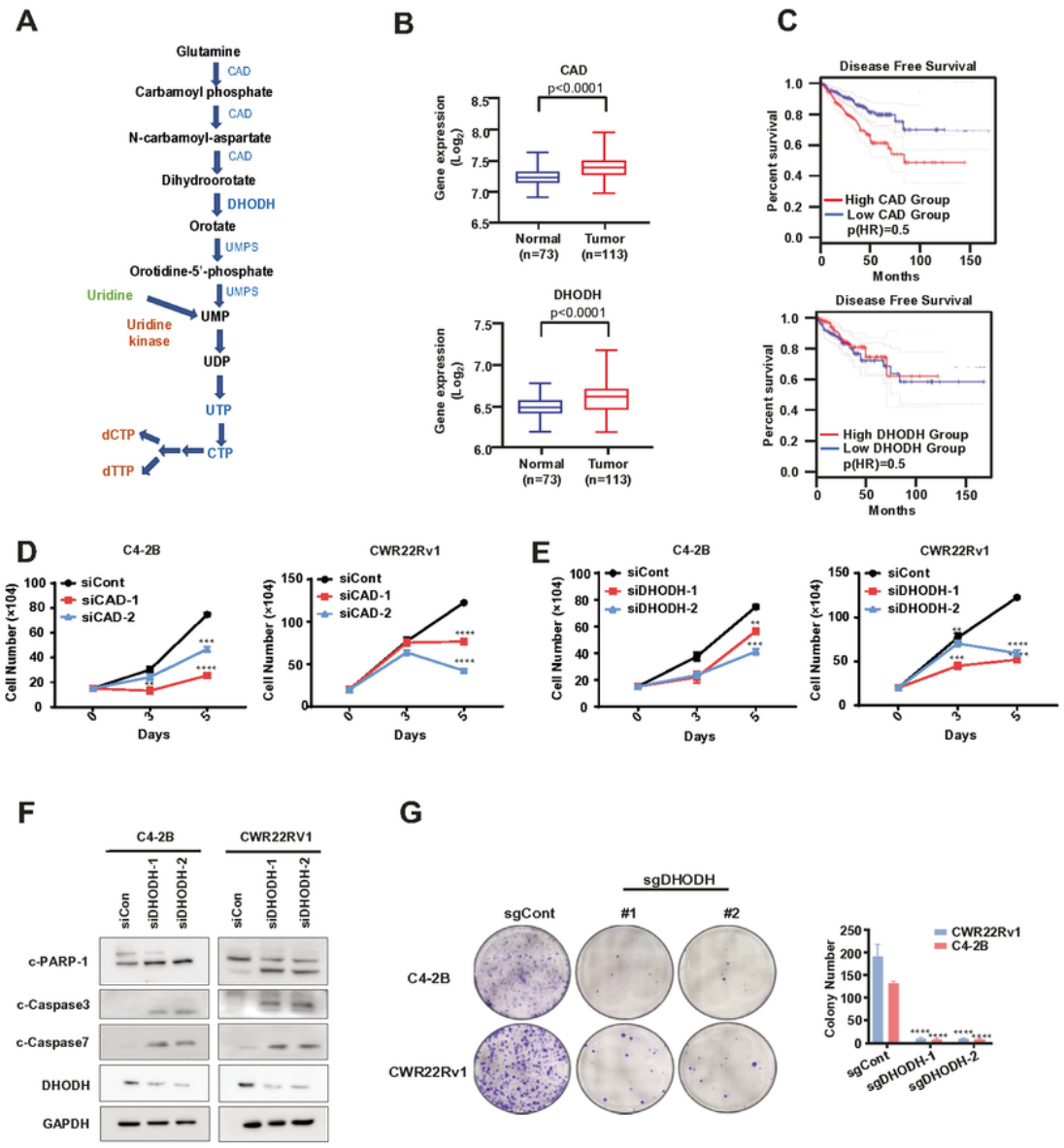

Figure 1

DHODH overexpression associates with CRPC and is a critical dependency of CRPC cell survival and proliferation. A Simplified schematic of *de novo* pyrimidine biosynthesis pathway. **B** Transcript levels of *CAD* and *DHODH* identified in tumor and normal tissues were estimated by The Cancer Genome Atlas (TCGA) database. **C** The association of *CAD* and *DHODH* expression with Prostate cancer patient outcomes from GEPIA 2. **D, E** C4-2B and CWR22Rv1cells were transfected with DHODH(CAD) or control

siRNA. After indicated times, C4-2B and CWR22Rv1 cell numbers were counted. **F** C4-2B and CWR22Rv1cells were transfected with DHODH or control siRNA. Two days later, DHODH, c-PARP-1, c-Caspase-3, c-Caspase-7 protein expression were detected by western blot. **G** C4-2B and CWR22Rv1 cells were infected with lentiviruses expressing two different shRNA against DHODH, and clone counts were performed 11 days later. Data shown are mean ± SD. Student's *t*-test. ** $p < 0.01$, *** $p < 0.005$, **** $p < 0.0001$, $n = 3$.

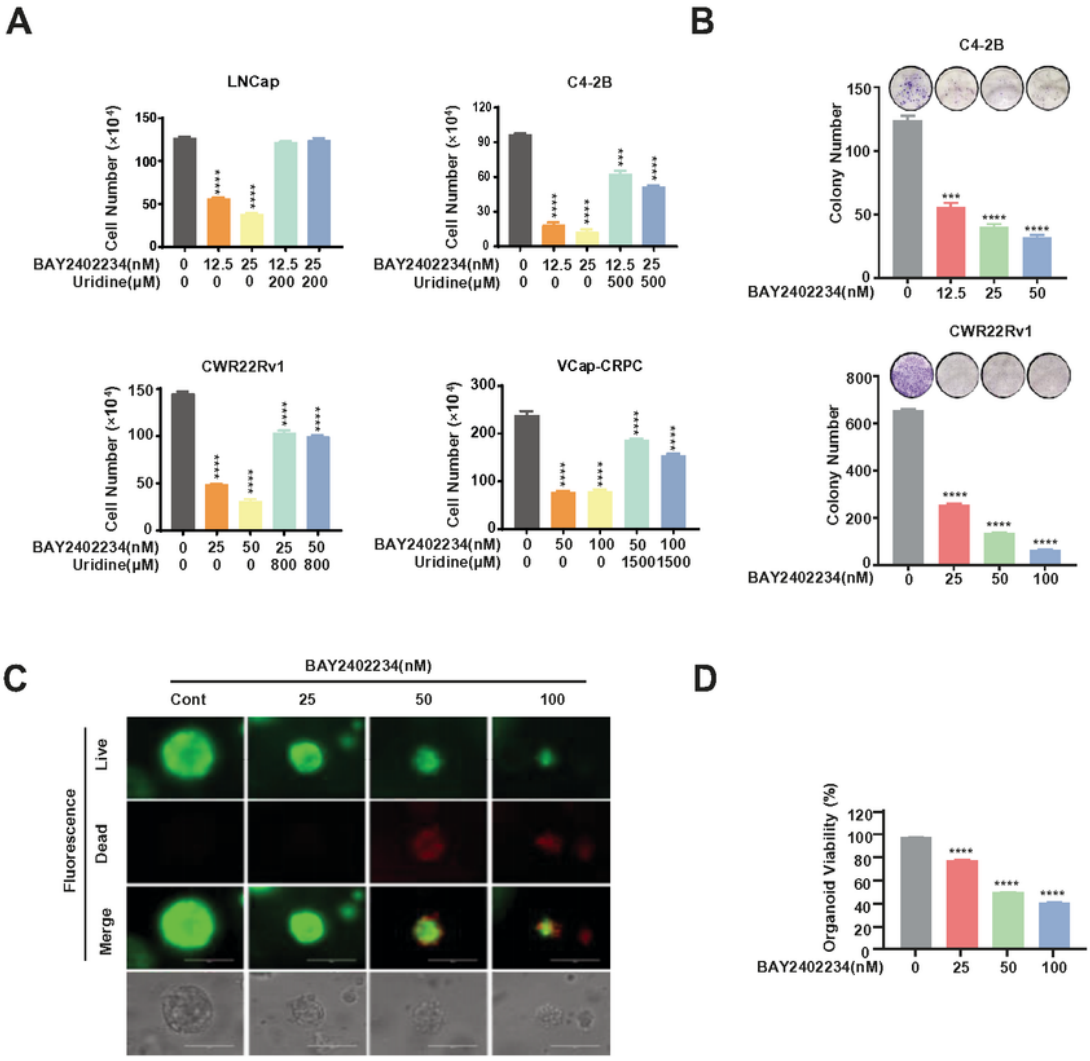

Figure 2

DHODH inhibitor inhibits proliferation and survival in CRPC cells. A Proliferation of prostate cancer cells treated with indicated dose of BAY2402234 as well as combination of BAY2402234 plus exogenous uridine. The dose of these two compounds were shown in the above. **B** The clonogenic ability of C4-2B and CWR22Rv1cells treated with indicated BAY2402234 was analyzed. **C, D** PDX-derived organoids were treated with vehicle (DMSO) or indicated concentrations of BAY2402234. **C** Four days later, representative images were taken by a fluorescence microscope. Scale bars, 20 μM. D After four days, the cell viability of organoids was detected by Cell-Titer-Glo. Data shown are mean ± SD. Data shown are mean ± SD. Student's *t*-test. *** $p < 0.005$, **** $p < 0.0001$, $n = 3$.

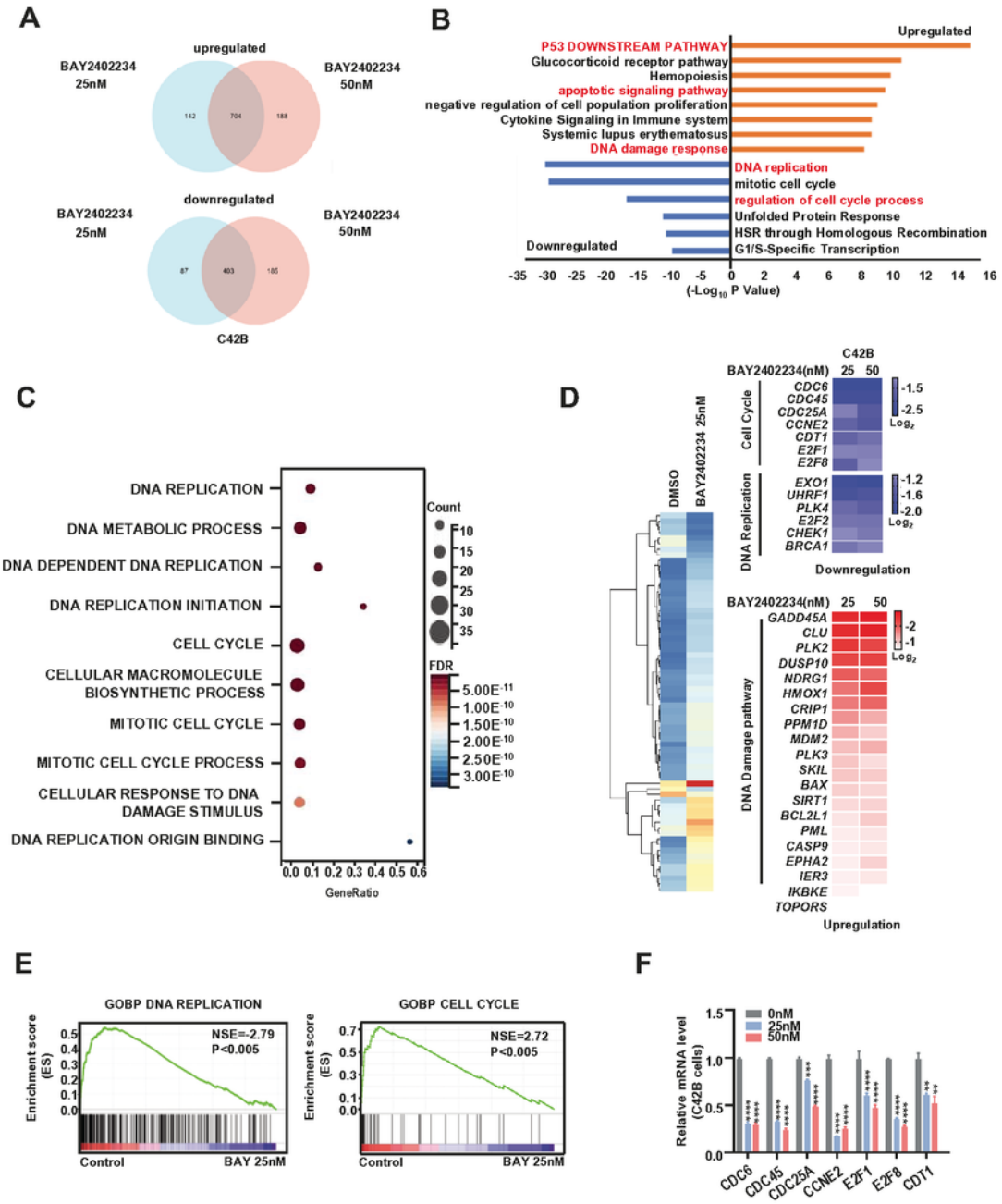

Figure 3

DHODH inhibition induces DNA damage, blocks the cell cycle and DNA replication in CRPC cells. A Venn diagram of the number of genes with expression significantly (1.5-fold) up-regulated or down-regulated, which was detected by RNA-seq of C4-2B cells treated with 25nM or 50nM BAY2402234 for 48h. **B** GSEA of top enriched gene sets in C4-2B cells treated with BAY2402234. The up-regulated and down-regulated gene sets from Hallmark and KEGG platforms were output by GSEA. **C** According to the RNA-seq

sequencing results of C4-2B cells cultured for 48 h under 25nM and 50nM BAY2402234 conditions, the significantly down-regulated signaling pathways were analyzed by KEGG and hallmark databases, and displayed in the form of bubble map. **D**Heatmap and hierarchical clustering displaying the fold changes of gene expression detected by RNA-seq in C4-2B cells treated with BAY2402234 (25nM and 50nM) for 48 hours, compared to vehicle (DMSO). Correctly display genes with log2 > 0.585 expression changes under at least one condition. Genes are displayed in rows, and the standardized count of each sample is displayed in columns. Red indicates up-regulated, and blue indicates down-regulated expression level. Middle and right, Cell cycle, DNA replication and DNA Damage signature genes that were altered in expression are displayed. **E**GSEA of the Cell Cycle and DNA Replication signatures in C4-2B cells treated with BAY2402234(25nM). The signature was defined by genes that significant expression changes by androgen stimulation in Prostate cancer cells. **F** qRT-PCR analysis of the indicated genes in C4-2B cells treated with DMSO or with BAY2402234(25nM or 50nM) for 48h. Data shown are mean ± SD. Student's *t*-test. ** $p < 0.01$, *** $p < 0.005$, **** $p < 0.0001$, $n = 3$.

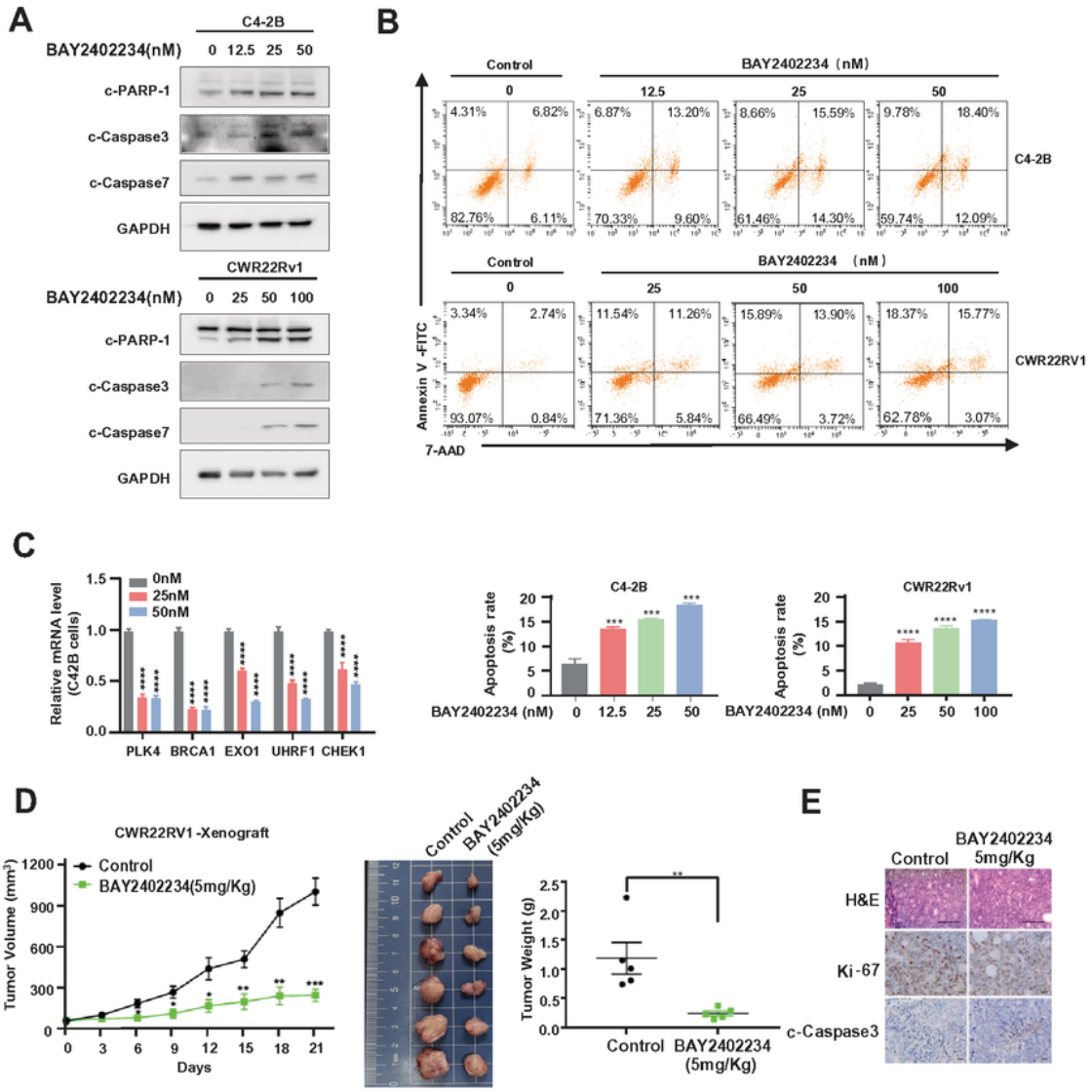

Figure 4

DHODH inhibitor exerts potent anti-tumor activity in CRPC *in vitro* and *in vivo*. AC4-2B and CWR22Rv1 cells were treated with vehicle (DMSO) or indicated BAY2402234 for 48 h. Indicated proteins were analyzed by western blot. **B** Apoptosis as measured by flow cytometry for Annexin and 7-AAD positive cells, respectively, in BAY2402234-treated C4-2B and CWR22Rv1 cells for 48 h. **C** qRT-PCR analysis of the indicated genes in C4-2B cells treated with DMSO or with BAY2402234(25nM or 50nM) for 48 hours. Data

shown are mean ± SD. Student's *t*-test, *** $p < 0.005$, **** $p < 0.0001$, $n = 3$. **D** Mice bearing CWR22Rv1 xenografts were administered BAY2402234 (5mg/Kg) by oral gavage once a day for 3 weeks. Tumor volumes were measured every other day. Then, the tumors were collected and weighted in each group. **E** H&E staining and immunohistochemical analysis of tumor tissues. H&E images, anti-Ki-67 and anti-cleaved caspase-3 IHC images of tumor sections were shown in above. Scale bars, 20 μm. Data shown are mean ± SD. Student's *t*-test, * $p < 0.05$, ** $p < 0.01$, *** $p < 0.005$, **** $p < 0.0001$, $n = 5$.

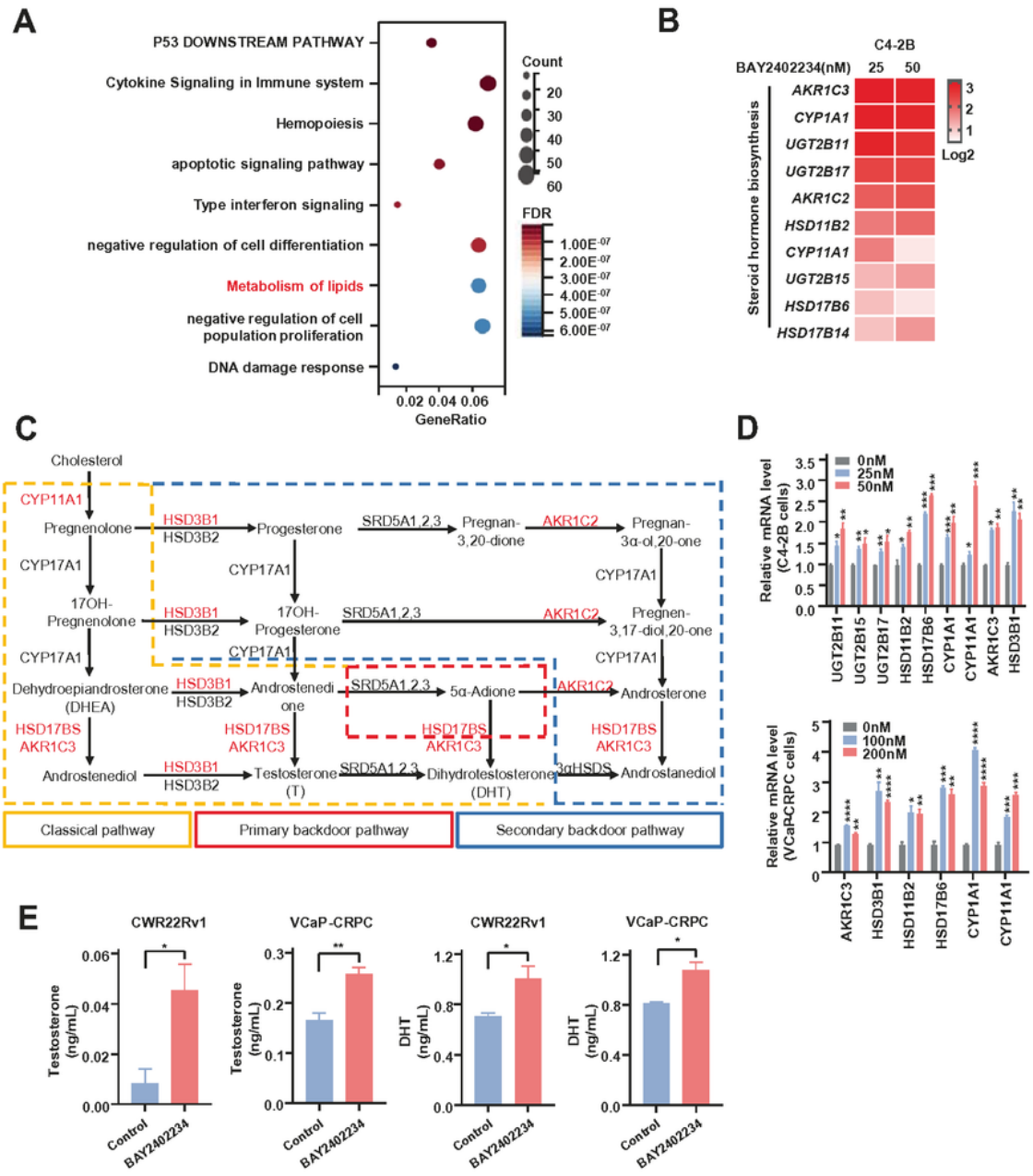

Figure 5

DHODH inhibition activates intracrine androgen biosynthesis pathway and AR signaling. A According to the RNA-seq sequencing results of C4-2B cells cultured for 48 h under 25nM and 50nM BAY2402234 conditions, the significantly up-regulated signaling pathways were analyzed by KEGG and hallmark databases, and displayed in the form of bubble map. **B** Heatmap displaying the fold changes of gene expression detected by RNA-seq in C4-2B cells treated with BAY2402234 (25nM and 50nM) for 48 hours, compared to vehicle (DMSO). Correctly display genes with log2 > 0.585 expression changes under at least one condition. Genes are displayed in rows, and the standardized count of each sample is displayed in columns. Red indicates up-regulated expression level. Steroid hormone biosynthesis signature genes that were altered in expression are displayed. **C** The diagram shows the classical (canonical or front-door) and alternative (back-door) pathways of androgen biosynthesis. Androgens are synthesized by cholesterol through a variety of enzymatic steps. CYP11A1 is responsible for the conversion of cholesterol to pregnenolone by side chain cleavage of cholesterol. CYP17A1 gene converts pregnenolone into dehydroepiandrosterone (DHEA) and androstenedione. The classical pathway of testosterone biosynthesis is that the main adrenal DHEA and androstenedione in the testis are converted to testosterone, and then testosterone 5α is reduced to dihydrotestosterone (DHT) by 5α-reductase (SRD5As). On the other hand, the synthesis of DHT by bypassing testosterone through the 5α-reduction of upstream steroids can be achieved through two other back-door pathways. In the primary backdoor pathway, 17OH-progesterone was reduced to 5α-and 3α-by SRD5As and AKR1C2 respectively before the 17,20-lyase reaction of CYP17A1 gene, and then reduced to androstenedione by HSD17Bs and AKR1C3. In the secondary backdoor pathway, androstenedione is converted to 5α-androstenedione (5α-Adione) by SRD5As, and then to DHT by HSD17Bs and AKR1C3. Through these back-door pathways, DHT is synthesized without the use of testosterone as an intermediate. **D** qRT-PCR analysis of the indicated genes in C4-2B and CWR22Rv1cells treated with DMSO or with BAY2402234 (25nM or 50nM) for 48 h. **E** LC-MS/MS measurement of T and DHT in VCaP-CRPC and CWR22Rv1 cells upon BAY2402234 treatment. Data shown are mean ± SD. Student's *t*-test, * $p < 0.05$, ** $p < 0.01$, *** $p < 0.005$, **** $p < 0.0001$, $n = 3$.

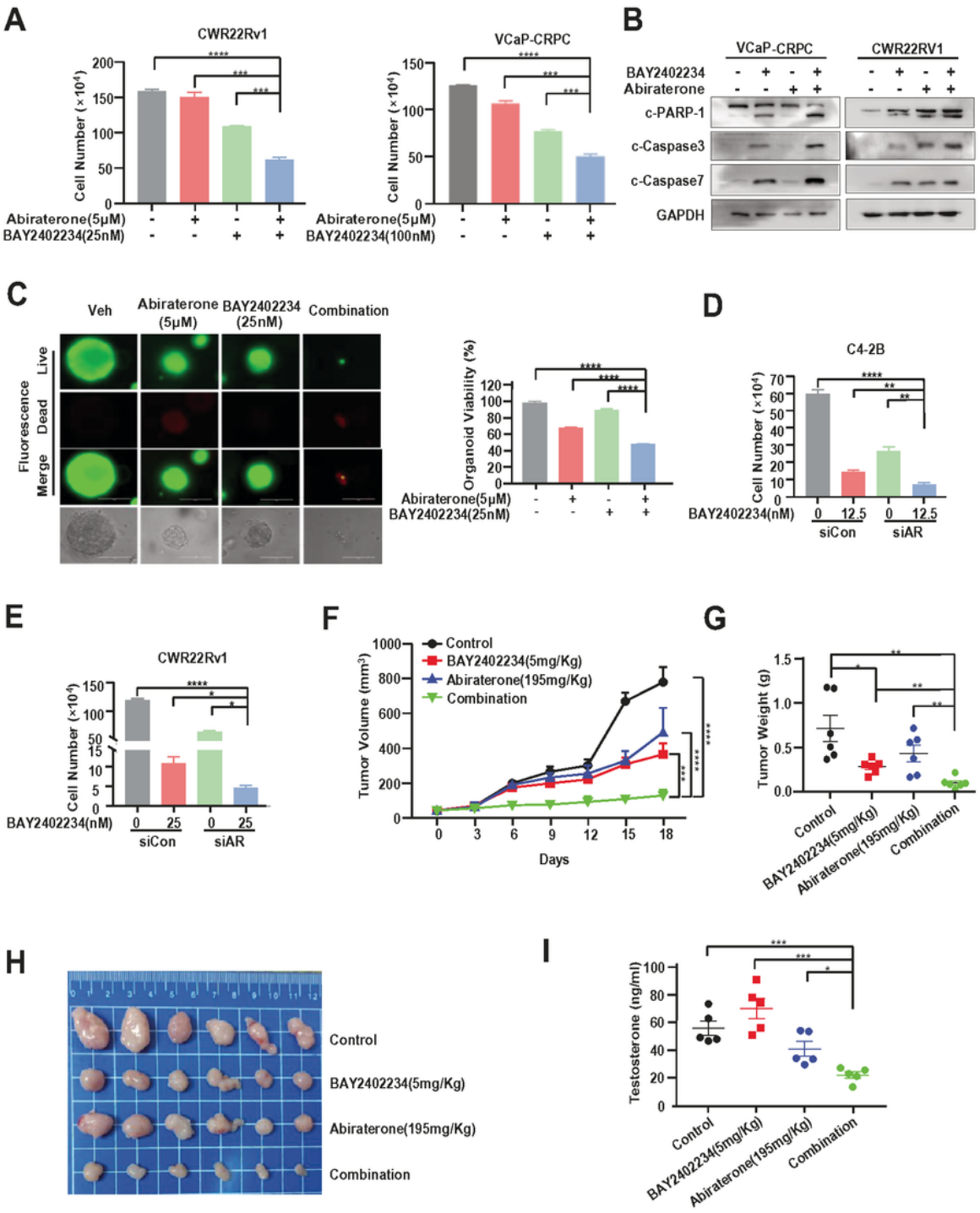

Figure 6

Combine DHODH inhibitor and abiraterone treatment adds sensitivity of CRPC inhibition and blocks intracrine androgen. A VCaP-CRPC and CWR22Rv1 cells were treated with BAY2402234 (25nM or 100nM) or abiraterone (5μM) alone or in combination. After 96 h, total cell numbers were counted. Data shown are mean ± SD. Student's *t*-test, *** $p < 0.005$, **** $p < 0.0001$, $n = 3$. **B** VCaP-CRPC and CWR22Rv1 cells were treated with BAY2402234 (25nM or 100nM) or abiraterone (5μM) alone or in combination. Indicated

proteins were detected by western blot after 48 hours. **C** PDX-derived organoids were treated with BAY2402234 (25nM) or abiraterone (5μM) alone or in combination. Four days later, representative images were taken by a fluorescence microscope. Scale bars, 20 μM. The cell viability of organoids was detected by Cell-Titer-Glo. **D, E** C4-2B and CWR22Rv1 cells were transfected with AR or control siRNA, follow by treated with DMSO or BAY2402234(12.5nM or 25nM). After 96 h, total cell numbers were counted. Data shown are mean ± SD. Student's *t*-test, * $p < 0.05$, ** $p< 0.01$, *** $p < 0.005$, **** $p < 0.0001$, $n = 3$. **F**Mice bearing CWR22Rv1 xenografts were treated with vehicle, BAY2402234 (5mg/Kg, p.o.), abiraterone (0.5mmol/Kg, i.p) or their combination for 18 days. Tumor volumes were measured every other day. Data shown are mean ± SD. Student's *t*-test, *** $p < 0.005$, **** $p < 0.0001$, $n = 5$. **G, H** The tumors were weighted in each group. Data shown are mean ± SD. Student's *t*-test, * $p < 0.05$, ** $p < 0.01$, $n = 6$. **I** LC-MS/MS measurement of T in tumor tissue. Data shown are mean ± SD. Student's *t*-test, * $p < 0.05$, *** $p < 0.005$, $n = 5$.

Supplementary Files

This is a list of supplementary files associated with this preprint. Click to download.

- SupplementaryFigurelegends.pdf
- Supplementary.pdf
- supplementarytable.xlsx